

Excitonic and Quasiparticle Life Time Effects on Silicon Electron Energy Loss Spectrum from First Principles

B. Arnaud

*Groupe Matière condensée et Matériaux (GMCM),
Campus de Beaulieu - Bat 11 A, 35042 Rennes Cedex, France, EU*

S. Lebègue and M. Alouani

*Institut de Physique et de Chimie des Matériaux de Strasbourg (IPCMS),
UMR 7504 du CNRS, 23 rue du Loess, 67034 Strasbourg, France, EU and
Max-Planck-Institut für Festkörperforschung, D-70506 Stuttgart, Germany, EU*

(Dated: November 14, 2018)

The quasiparticle decays due to electron-electron interaction in silicon are studied by means of first-principles all-electron GW approximation. The spectral function as well as the dominant relaxation mechanisms giving rise to the finite life time of quasiparticles are analyzed. It is then shown that these life times and quasiparticle energies can be used to compute the complex dielectric function including many-body effects without resorting to empirical broadening to mimic the decay of excited states. This method is applied for the computation of the electron energy loss spectrum of silicon. The location and line shape of the plasmon peak are discussed in detail.

PACS numbers: 71.15.Mb, 71.35.-y, 78.20.-e, 79.20.Uv

One of the most challenging condensed matter problems is the prediction of excited states of materials from first principles[1]. The solution of this formidable task is doubly rewarding since (1) most of the interesting physics involves the interaction of an electromagnetic radiation with matter, and (2) most of progress in today's nanoelectronic technologies requires the knowledge of excited states.

In the last few decades, the development of this field has been expending rapidly, and several evolutionary periods can be distinguished. In the first one, the density functional theory in the local density approximation (LDA) played a major role, and was widely used for the analysis of spectroscopic properties of materials[2, 3], despite that the band gaps of semiconductors and insulators were adjusted by *ad hoc* methods. Later, it was realized that the GW approximation of Hedin[4] provides a practical scheme for the determination of the quasiparticle energies, and band gaps were no longer adjusted[5]. Nevertheless, even the use of correct band gaps and the various types of exchange-correlation corrections, including local-field effects, did not improve significantly the calculated optical spectra[2]. It was often believed that the inclusion of the electron-hole (*e-h*) interactions was the missing ingredient for an adequate description of the optical spectra, and this was later confirmed by model calculations[6]. However, it is only recently that *ab initio* methods explicitly showed the relevance of these complex interactions to the calculation of the dielectric function[1]. At this point, calculations from first-principles were finally making direct contact with experiment and establishing the relevance of the *e-h* interactions.

The aim of this Letter is to add a further step to this fascinating development by incorporating, from first principles and for the first time, the life time of inter-

band transitions into the calculation of the dielectric function. As a consequence an empirical broadening is no longer needed for a successful comparison of theoretical and experimental optical spectra. This work also improves upon existing excited state calculations based on the pseudopotential (PP) approach in conjunction with plasmon-pole (PIP) models for the screening of the Coulomb interaction[1]. In those types of calculations not only the various types of matrix elements of operators are not accurate due to the use of pseudowave functions, the PIP approximation also makes it impossible to determine the imaginary part of the self-energy, and hence the spectral functions and life times of quasiparticles remain unaccessible. Indeed, it has been noticed recently[7, 8, 9] that GWA implementations based on PP methods led to larger and more \mathbf{k} -dependent shifts than those based on all-electron methods. To illustrate our method, we compute the plasmon resonance and the line shape of the electron energy loss spectrum (EELS) of silicon, one of the most used materials in today's technology.

The most successful approach for describing elementary excitations probed by photoemission experiments uses many-body Green's function theory. The energies and life times of quasiparticles are mainly determined by the pole structure of the Green's function G or more conveniently by solving the quasiparticle equation[10]. The self-energy operator $\Sigma = \Sigma^{(1)} + i\Sigma^{(2)}$ of the quasiparticles is non-local, frequency-dependant, and generally non hermitian. The non-hermitian part $i\Sigma^{(2)}$ is related to the dominant relaxation mechanisms (scattering on crystal imperfection, electron-phonon or electron-electron interaction) which give rise to the finite life time of quasiparticles. In the present work, Σ is computed within Hedin's GW framework[4] which includes dynamic polarization in the random-phase approximation (RPA). In such an approach, only the electron-electron interaction

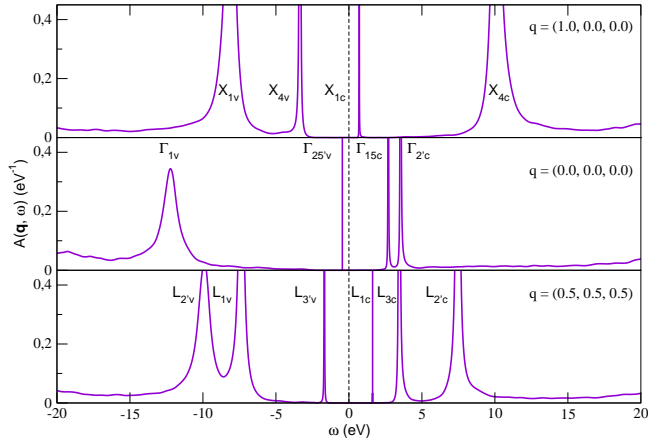


FIG. 1: Spectral function of silicon for L , Γ and X \mathbf{k} points. The \mathbf{q} vectors are given in units of $2\pi/a$, where $a = 10.261$ a.u. The energy zero is fixed at the energy of the topmost occupied LDA state at the Γ point.

contributes to the non-hermitian part of the self-energy, i.e to the instability of single-particle excitation.

The complex QP energies $\epsilon_{n\mathbf{k}}^{qp}$ are solutions of the quasiparticle equation for a state labeled $n\mathbf{k}$, and are in practice obtained using a first order perturbation theory[5]. The real part of $\epsilon_{n\mathbf{k}}^{qp}$ corresponds to the QP energy, and the life time of a single-particle excitation, given by the inverse of the full-width at half-maximum (FWHM) of the QP peak in the spectral function, is defined by $\tau_{n\mathbf{k}} = [2 \times |\Gamma_{n\mathbf{k}}|]^{-1}$ where $\Gamma_{n\mathbf{k}} = \text{Im}[\epsilon_{n\mathbf{k}}^{qp}]$. The determination of both QP energies and their life times requires the computation of the self-energy matrix elements[11].

The LDA eigenvalues and eigenvectors obtained by means of the all-electron Projector Augmented-Wave method[12] are used as a starting point for our GWA calculations. The wave functions are expanded into plane-waves up to 20 Ry and three partial waves of s , p and d types are used to describe the correct nodal structure of the wave functions near the nuclei.

In Fig. 1 the spectral function of some selected high symmetry \mathbf{k} -points (L , Γ , X) of silicon is displayed. The FWHM of the QP peaks increases almost linearly away from the band gap because more and more decay channels of Auger type become available. Physically speaking, a QP is scattered into LDA empty states whose energies are between the QP energy and the Fermi energy.

The GW self-consistency should affect the QP life time. Indeed, the number of decay channels of Auger type is fixed by the smallest possible excitation energy contained in the screened interaction $\tilde{W}(\omega)$ which is defined by the absolute band gap of silicon. As the band gap increases from 0.44 eV to 1.0 eV when going from the LDA to the GW approximation (see Fig. 2.a), we expect a decrease of the imaginary part of the self-energy caused by self-consistent effects. Therefore the QP peak should be narrowed, corresponding to increased life times. Another

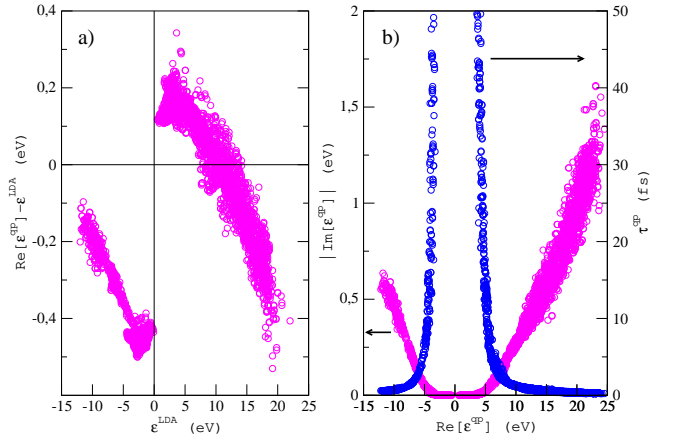


FIG. 2: (a) Shifts of QP peak positions $\text{Re}[\epsilon^{qp}] - \epsilon^{LDA}$ of silicon as function of the LDA energies ϵ^{LDA} for the first 16 bands and for 216 \mathbf{k} -points sampling the full Brillouin zone. (b) Imaginary part $|\text{Im}(\epsilon^{qp})|$ and life times τ^{qp} of QPs as a function of the QP peak positions. The energy zero is fixed at the topmost occupied LDA state at the Γ point.

consequence of the lack of self-consistency is that some states near the Fermi level have a spurious imaginary part because they fall between the LDA and GW Auger thresholds. Thus, the life times of the QPs in the vicinity of the gap are not correct except at the uppermost valence state and at the lowest conduction states where the non-hermitian part of the self-energy due to phonons is strictly zero[13]. A proper description of the QP life time in this range of energy should include the interaction of electronic states with lattice vibrations because the dominant relaxation process is governed by electron-phonon interaction. We expect, however, that our predictions are quantitatively correct at high energy where the dominant relaxation mechanism is electron-electron interaction. Therefore, the complex QP energies obtained by means of the GW approximation represent a good starting point for the direct calculation of the complex dielectric function at high energy without using any phenomenological life time of excited states.

To include the e - h interaction in the dielectric function we solve the Bethe-Salpeter equation, which describes the propagation of a correlated quasielectron-quasihole pair, and can be turned into an effective two-particle Schrödinger Hamiltonian whose block matrix form is given by

$$H^{\text{exc}} = \begin{pmatrix} R & C \\ -C^* & -R^* \end{pmatrix}. \quad (1)$$

Detailed expressions of the different block matrix elements can be found elsewhere[14]. The diagonal blocks given by R and $-R^*$ are respectively the resonant part ($v\mathbf{k} \rightarrow c\mathbf{k}$ transitions) and the anti-resonant part ($c\mathbf{k} \rightarrow v\mathbf{k}$ transitions) while the off-diagonal blocks C and $-C^*$ couple positive and negative frequency transitions. Olivano and Reining have shown that these off-diagonal

blocks are crucial for the correct description of the EELS of silicon[15]. Here, we follow a similar approach, but in contrast to their work, we include the life time of non-interacting e - h pairs by considering complex transition energies whose imaginary part is set by $\text{Im}[\epsilon_{\mathbf{c}\mathbf{k}}^{qp} - \epsilon_{\mathbf{v}\mathbf{k}}^{qp}] =$

$\Gamma_{\mathbf{c}\mathbf{k}} - \Gamma_{\mathbf{v}\mathbf{k}}$. Therefore, even if one neglects the off-diagonal blocks, the effective Hamiltonian H^{exc} is non-hermitian because the diagonal matrix elements of R are complex.

The macroscopic dielectric function is given by

$$\epsilon(\mathbf{q} = \mathbf{0}, \omega) = 1 - \lim_{\mathbf{q} \rightarrow \mathbf{0}} \frac{4\pi}{\Omega} \times \frac{1}{\mathbf{q}^2} \times \sum_{n_1, n_2, n_3, n_4} \langle n_1 | e^{-i\mathbf{q}\cdot\mathbf{r}} | n_2 \rangle \times [H^{\text{exc}} - \omega I]_{(n_1, n_2), (n_3, n_4)}^{-1} \times \langle n_4 | e^{i\mathbf{q}\cdot\mathbf{r}} | n_3 \rangle \times (f_{n_4} - f_{n_3}), \quad (2)$$

with f_{n_i} being the occupation number of the Bloch state labeled by n_i and with $(n_i, n_j) = (\mathbf{v}\mathbf{k}, \mathbf{c}\mathbf{k})$ or $(\mathbf{c}\mathbf{k}, \mathbf{v}\mathbf{k})$.

To build the excitonic Hamiltonian H^{exc} , we first calculate the complex QP energies for the first 16 bands and for the 216 \mathbf{k} points sampling the Brillouin zone. Fig. 2.a shows the shifts of the real part of the QP energies with respect to the LDA energies as a function of LDA energies. Interestingly, these shifts are far from being uniform across the BZ with the exception of LDA states ranging from -5 eV to 5 eV. In this range of energy, the valence LDA states are shifted downward by about 0.45 eV while the LDA conduction states are shifted upward by about 0.15 eV. The striking feature is the decrease of the QP energy shifts for the LDA conduction states above 5 eV. This trend was also observed by Fleszar and Hanke[16]. In addition, the QP shifts below -5 eV reflect the contraction of the occupied GW bandwidth with respect to that of the LDA. Such a contraction is *not* observed when using a plasmon-pole model. Fig. 2.b shows the imaginary part of the QP as a function of the QP peak positions. It's worth mentioning that the imaginary part of the QP of Ref. [16] are twice as larger as ours. Such a large difference can certainly be ascribed to the value of the broadening parameter δ used in Ref. [16] to evaluate $\tilde{W}(\omega)$ along the real axis (see Ref. [7] for details). The broadening should be chosen as small as possible ($\delta \rightarrow 0$) to obtain correct life times. Notice that $|\text{Im}(\epsilon_{n\mathbf{k}}^{qp})|$ is very small for the QP states ranging from -5 eV to 5 eV and increases almost linearly outside this interval. Thus, we expect a non negligible broadening $|\Gamma_{\mathbf{c}\mathbf{k}} - \Gamma_{\mathbf{v}\mathbf{k}}|$ of about 0.5 eV for non interacting transition energies in the range of energy where the plasmon resonance occurs.

Fig. 3 shows our calculated EELS ($-\text{Im}[\epsilon^{-1}(\mathbf{q} = \mathbf{0}, \omega)]$) of silicon[17]. These results are compared with the experimental spectrum[18] characterized by a rather symmetric plasmon peak located at 16.7 eV. The dashed line represents the spectrum calculated within the RPA approximation which amounts to retaining just the complex transition energies in the excitonic Hamiltonian. The main peak of the RPA spectrum is shifted by about 1 eV towards higher energy compared to experiment. In addition, the FWHM of the plasmon peak $\Delta E_{\frac{1}{2}}$ is underestimated by a factor of 3 while the height is overestimated by the same factor. When including both e - h at-

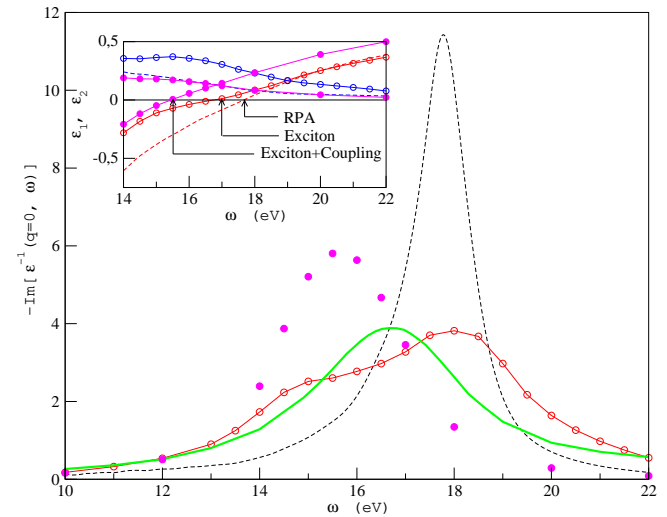


FIG. 3: EELS of silicon: the thick line is the experimental data by Stiebling (Ref. [18]), the dashed line is the RPA calculation without excitonic effects (local-field effects are also neglected), the curve with empty circles includes both excitonic effects and local-field effects, while the full circle curve is same as empty circle one but includes the coupling. The complex GW eigenvalues have been used in all calculations. The real part ϵ_1 and imaginary part ϵ_2 of the dielectric function are shown in the inset (Arrows show the zero of $\epsilon_1(\omega)$).

traction and local-field effects but still neglecting the coupling between positive and negative frequency transitions (open circles), the line shape of the spectrum worsens. The plasmon-peak position is now ill-defined because the spectrum exhibits two structures located at 15 and 18 eV. Finally, the inclusion of the coupling between forward and backward going quasihole-quasielectron pairs by taking into account the off-diagonal blocks of H^{exc} has a rather drastic effect on the overall spectrum (full circles). On the one hand, the natural line shape is improved and, as expected, $\Delta E_{\frac{1}{2}} \simeq 3$ eV is underestimated with respect to experiment ($\simeq 3.7$ eV) because of the analyzer resolution included in the latter. On the other hand, the main peak of our spectrum is unfortunately shifted, by about 1 eV, towards lower energy compared to experiment, and its height is somehow overestimated.

However, the inclusion of the analyzer resolution would slightly reduce the calculated height.

The position of the plasmon peak ω_p is determined roughly by the zero of the real part $\epsilon_1(\omega)$ of the macroscopic dielectric function. The inset in Fig. 3 clearly shows the shift of the zero towards lower energies when the excitonic effects and coupling terms are included. It's also of interest to notice that the FWHM of the plasmon peak is qualitatively given by $\Delta E_{\frac{1}{2}} \simeq 2 \times \epsilon_2(\omega_p) / \frac{\partial \epsilon_1(\omega)}{\partial \omega} |_{\omega_p}$. Thus $\Delta E_{\frac{1}{2}}$ is controlled by the value of ϵ_2 at the plasmon resonance energy and by the slope of ϵ_1 at the same energy as it can be seen in Fig. 3. For example, a detailed comparison of both calculations, where the exchange-correlation effects are taken into account, shows that the inclusion of the coupling yields a decrease in ϵ_2 as well as an increase in the slope of ϵ_1 , i.e., it leads to a narrowing of the plasmon peak.

Obviously, the puzzling feature of our calculated spectrum is the underestimation of the plasmon-peak energy. It is therefore worth comparing our findings to the only available PP results[15]. The PP plasmon peak is located at about 17.3 eV while ours is located at 15.7 eV. These differences arise because we avoid most of the approximations used in Ref. 15. In particular, (1) we avoid using PP methods, and any kind of plasmon-pole model to calculate QP energies (such models are expected to fail at these high energies), (2) we don't use any broadening parameter to describe the life times of excited states, and

finally (3) we avoid using first order perturbation theory to include the coupling between positive and negative frequency transitions. This latter approximation is shown to have only a minor effect on the final spectrum [15]. As a consequence of the first two approximations, their plasmon-peak energy position, at the RPA level without excitonic effects, is already shifted by 0.9 eV towards higher energies with respect to ours. A self-consistent GW calculation[9] should improve the agreement with experiment by enlarging the transition energies. However, self-consistency issues are beyond the scope of this work.

In conclusion, we have calculated the QP energies and life times of silicon within the all-electron GW approximation. We have also demonstrated that these QP energies can be used to evaluate the EELS of silicon without using any phenomenological parameter to describe the life times of excited states. Our results confirm that it is crucial to include excitonic effects and coupling between forward and backward going e - h pairs to obtain an improved line shape. However, the underestimation of the plasmon-peak position reflects the need for a self-consistent calculation of the QP energies or the need for an approximation beyond the GW method.

We are grateful to V. Olevano for providing us with some details about his calculations. The supercomputer time has been granted by CINES (Project No. gmg2309) on the IBM SP4.

-
- [1] G. Onida *et al.*, Rev. Mod. Phys. **74**, 601 (2002) and references therein.
- [2] S. Louie *et al.*, Phys. Rev. Lett. **34**, 155 (1975), Z. H. Levine, and D. C. Allan, Phys. Rev. Lett. **66**, 41 (1991).
- [3] S. Baroni and R. Resta, Phys. Rev. B **33**, 7017 (1986), M. Alouani and J. M. Wills, Phys. Rev. B. **54**, 2480 (1996), V. I. Gavrilenko and F. Bechstedt, Phys. Rev. B **55**, 4343 (1997).
- [4] L. Hedin, Phys. Rev. **139**, A796 (1965).
- [5] M. S. Hybertsen and S. G. Louie, Phys. Rev. B **34**, 5390 (1986).
- [6] W. Hanke and L. J. Sham, Phys. Rev. B **21**, 4656 (1980); M. del Castillo-Mussot and L. J. Sham, Phys. Rev. B **31**, 2092 (1985), see also L. J. Sham and T.M. Rice, Phys. Rev. **144**, 708 (1966) and G. Strinati, Phys. Rev. Lett. **49**, 1519 (1982); Phys. Rev. B **29**, 5718 (1984).
- [7] S. Lebègue, B. Arnaud, M. Alouani, and P. Bloechl, Phys. Rev. B (accepted).
- [8] B. Arnaud and M. Alouani, Phys. Rev. B **63**, 085208 (2001).
- [9] W. Ku and A. G. Equiluz, Phys. Rev. Lett. **89**, 126401 (2002).
- [10] A. J. Layzer, Phys. Rev. **129**, 897 (1963).
- [11] Both the screened interaction \tilde{W} and the self-energy Σ_c are evaluated in reciprocal space with an adequate \mathbf{k} point sampling ($6 \times 6 \times 6$ mesh), and 137 \mathbf{G} reciprocal space vectors. For the Hartree-Fock contribution to the self-energy we used 283 \mathbf{G} vectors, because of the slow convergence as a function of \mathbf{G} . The screening matrix \tilde{W} was calculated at a discrete mesh of energies ranging from 0 to 100 eV with a step of 0.5 eV. A linear interpolation scheme between energy-mesh points to the actual energy argument $|\epsilon_{n\mathbf{k}} - \omega|$ was applied for each matrix element. The integral over the imaginary energy-axis was performed by a Gaussian quadrature (11 points are found sufficient to obtain well converged quantities because of the smoothness of the integrand along the imaginary energy-axis).
- [12] P.E Blöchl, Phys. Rev. B **50**, 17953 (1994).
- [13] P. Lautenschlager, P. B. Allen, and M. Cardona, Phys. Rev. B **33**, 5501 (1986).
- [14] M. Rohlfing and S. G. Louie, Phys. Rev. B **62**, 4927 (2000).
- [15] V. Olevano and L. Reining, Phys. Rev. Lett. **86**, 5962 (2001).
- [16] A. Fleszar and W. Hanke, Phys. Rev. B **56**, 10228 (1997).
- [17] Once the effective excitonic Hamiltonian H^{exc} has been constructed (matrix 20736×20736), a matrix inversion for each frequency ω is performed to obtain the macroscopic dielectric function $\epsilon(\mathbf{q} = \mathbf{0}, \omega)$ given by Eq. 2.
- [18] J. Stiebling, Z. Phys. B **31**, 355 (1978).